Composite active site of chondroitin lyase ABC accepting both epimers of uronic acid

Shaya, D.; Hahn, Bum-Soo; Bjerkan, Tonje Marita; Kim, Wan Seok; Park, Nam Young; Sim, Joon-Soo; Kim, Yeong-Shik.; Cygler, M.

National Research Council Canada   Conseil national de recherches Canada

Canada

Composite active site of chondroitin lyase ABC accepting both epimers of uronic acid

D. Shaya[2], Bum-Soo Hahn[3], Tonje Marita Bjerkan[4],
Wan Seok Kim[5], Nam Young Park[6], Joon-Soo Sim[6],
Yeong-Shik Kim[6], and M. Cygler[1,2,7]

[2]Department of Biochemistry, McGill University, Montréal, Québec,
Canada; [3]National Institute of Agricultural Biotechnology, 225 Seodun-Dong,
Suwon 441-707, South Korea; [4]Department of Biotechnology, The Norwegian
University of Science and Technology, Sem Sælands vei 6/8, N-7491
Trondheim, Norway; [5]Division of Hematology, St. Mary's Hospital, The
Catholic University of Korea, Seoul 150-713; [6]Natural Products Research
Institute, College of Pharmacy, Seoul National University, Seoul 110-460,
South Korea; and [7]Biotechnology Research Institute, NRC, 6100 Royalmount
Avenue, Montréal, Québec, H4P 2R2, Canada

**Enzymes have evolved as catalysts with high degrees of
stereospecificity. When both enantiomers are biologically
important, enzymes with two different folds usually cat-
alyze reactions with the individual enantiomers. In rare
cases a single enzyme can process both enantiomers effi-
ciently, but no molecular basis for such catalysis has been
established. The family of bacterial chondroitin lyases ABC
comprises such enzymes. They can degrade both chondroitin
sulfate (CS) and dermatan sulfate (DS) glycosaminoglycans
at the nonreducing end of either glucuronic acid (CS) or its
epimer iduronic acid (DS) by a β-elimination mechanism,
which commences with the removal of the C-5 proton from
the uronic acid. Two other structural folds evolved to per-
form these reactions in an epimer-specific fashion: $(\alpha/\alpha)_5$ for
CS (chondroitin lyases AC) and β-helix for DS (chondroitin
lyases B); their catalytic mechanisms have been established
at the molecular level. The structure of chondroitinase ABC
from *Proteus vulgaris* showed surprising similarity to chon-
droitinase AC, including the presence of a Tyr-His-Glu-
Arg catalytic tetrad, which provided a possible mechanism
for CS degradation but not for DS degradation. We deter-
mined the structure of a distantly related *Bacteroides thetaio-
taomicron* chondroitinase ABC to identify additional struc-
turally conserved residues potentially involved in catalysis.
We found a conserved cluster located ∼12 Å from the cat-
alytic tetrad. We demonstrate that a histidine in this cluster
is essential for catalysis of DS but not CS. The enzyme utilizes
a single substrate-binding site while having two partially
overlapping active sites catalyzing the respective reactions.
The spatial separation of the two sets of residues suggests
a substrate-induced conformational change that brings all
catalytically essential residues close together.**

Keywords: catalytic mechanism/chondroitinase ABC/crystal
structure/glycosaminoglycans/site-directed mutagenesis

[1]To whom correspondence should be addressed: Tel: +1-514-496-6321;
Fax: +1-514-496-5143; e-mail: mirek@bri.nrc.ca

Introduction

Enzymes acting on chiral substrates catalyze reactions with an
extremely high degree of stereospecificity that is associated
with preferential stabilization of one stereoisomeric transition
state over another (reviewed in Lamzin et al. (1995)). In many
instances enzymes with different topologies have evolved to
process two enantiomeric substrates. Some examples include
L- and D-amino acid oxidases (Pawelek et al. 2000), 2-hydroxy
acid dehydrogenases (Lamzin et al. 1994), and glycosaminogly-
can (GAG) lyases (Ernst et al. 1995). The active sites of such
enzyme pairs can show a near mirror symmetry embedded in
dissimilar folds (Lamzin et al. 1994; Mattevi et al. 1996). A dif-
ferent category of enzymes, racemases and epimerases, evolved
to catalyze inversions of stereochemistry (reviewed in Tanner
(2002)), and there is a good understanding of their catalytic
mechanism (Allard et al. 2001; Tanner 2002). In rare cases an
enzyme posses the ability to accept substrates with either config-
uration at the active center and convert them into new molecules.
For example, acetolacetate decarboxylase possesses the unique
ability to process both enantiomers of acetolacetate yielding
a single decarboxylation product enantiomer (Najmudin et al.
2003). Heparin lyase II (Shaya et al. 2006) and chondroitin
lyase ABC can depolymerize specific glycosaminoglycans by
abstracting C-5 proton from either side of their uronic acid
building block (Huang et al. 2003). However, the mechanistic
and structural details by which these enzymes perform these
tasks are presently not known. Here we address these ques-
tions for the uronic acid, epimer-nonspecific glycosaminoglycan
lyases.

Chondroitin sulfate (CS) and dermatan sulfate (DS), one of
the four classes of glycosaminoglycans, are linear, heteroge-
neous, highly negatively charged polysaccharides composed
of β(1→4)-linked disaccharide repeating units contain-
ing uronic acid (1→3) linked to *N*-acetyl-D-galactosamine
(GalNAc) (Ernst et al. 1995). The uronic acid moiety in
CS is exclusively β-D-glucuronic acid (GlcA), whereas DS
contains a mixture of α-L-iduronic acid (IdoA) and GlcA
epimers (Figure 1). GAGs linked via specific serine residues
to core proteins form proteoglycans (PGs), which are the ma-
jor components of the extracellular matrix of vertebrates. PGs
modulate fundamental biological processes such as cell ad-
hesion, proliferation, differentiation, signaling, inflammation,
and infection (Folkman and Klagsbrun 1987; D'Amore 1990;
Vlodavsky et al. 1991; Varki 1993; Bernfield et al. 1999; Bao
et al. 2004).

Bacterial GAG-degrading lyases depolymerize their sub-
strates through a β-elimination mechanism characterized by
charge neutralization of the carboxylic acid group, removal of
a relatively acidic proton from the C-5 carbon (chiral center) of
the uronic acid, and the release of the 4-linked hexosamine with
the generation of a C-4–C-5 double bond at the uronic acid ring
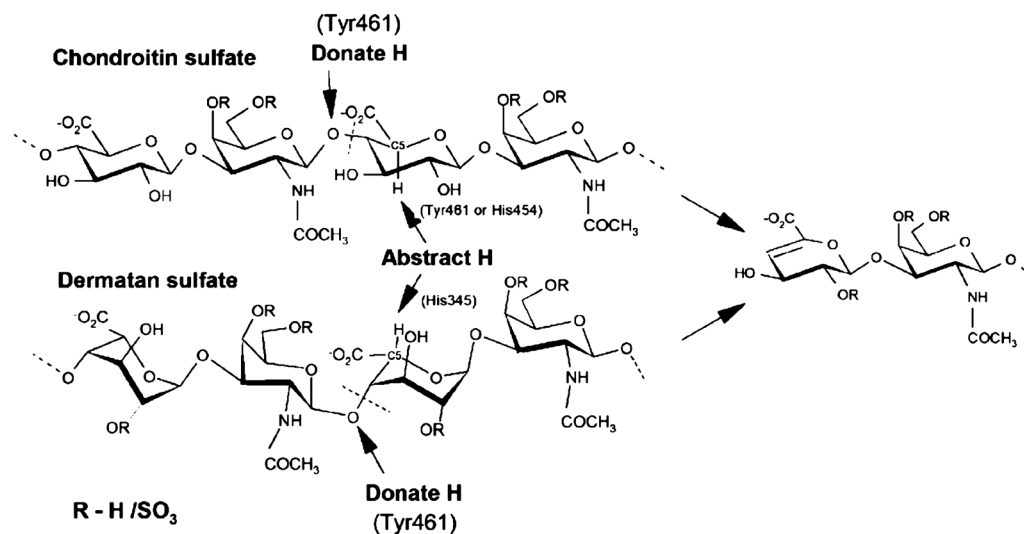(Gacesa 1987) (Figure 1).

Fig. 1. Lytic degradation of CS (top) and DS (bottom) by chondroitinase ABC I. Dashed line between the galactose and uronic acid indicates the bond that is being broken.

Enzymes with two distinct structural topologies have evolved to sterospecifically degrade either CS or DS. Chondroitin lyase AC (chondroitinase AC, chonAC), which specifically depolymerizes the glucuronic acid-containing CS (Figure 1, top), has a catalytic domain characterized by an incomplete $(\alpha/\alpha)_5$ toroid fold (Féthière et al. 1999). The crystal structures of chonAC from *Pedobacter heparinus* (PedAC) and *Arthrobacter aurescens* (ArthroAC) complexed with inhibitors and substrates (Huang et al. 2001; Lunin et al. 2004), combined with mutagenesis (Capila et al. 2002; Rye et al. 2006) showed that the enzyme utilizes an asparagine to neutralize the acidic group of GlcA (low-barrier hydrogen bond) and a Tyr-His-Glu-Arg hydrogen-bonded tetrad as a catalytic center. The role of the general base removing the glucuronic acid C-5 proton was assigned to a tyrosine in a deprotonated state (Lunin et al. 2004). The structural and biochemical data (Rye et al. 2006) argued for the same tyrosine to protonate also the leaving group, acting as a general acid. In contrast, chondroitin lyase B (chondroitinase B, chonB), which degrades exclusively iduronic acid-containing regions of DS (Figure 1, bottom), has a right-handed β-helix fold (Huang et al. 1999) similar to that of pectate and pectin lyases (Herron et al. 2003). This enzyme utilizes a Ca^{2+} ion coordinated by two glutamates and one asparagine to neutralize the acidic group of IdoA, whereas its catalytic center contains a lysine acting as a base abstracting the C-5 proton and an arginine performing the role of a general acid during catalysis (Michel et al. 2004).

In addition to these C-5 epimer-specific enzymes, another class of enzymes-designated chondroitin lyases ABC (chondroitinase ABC, chonABC) possesses the ability to degrade both CS and DS. Two isomers PvulABCI and PvulABCII were identified in the bacterium *Proteus vulgaris* and biochemically characterized (Hamai et al. 1997). Their sequences show no recognizable similarity to either chonAC or chonB. Nevertheless, the structure of PvulABCI revealed a very similar fold to chonAC, supplemented with an additional N-terminal domain (Huang et al. 2003). The similarity extends to the active site: PvulABCI contains an identical Tyr-His-Glu-Arg tetrad arrangement as that found in chonAC; their involvement in

catalysis was confirmed by mutagenesis (Prabhakar et al. 2005). Thus, the unusual ability of chonABC to abstract the proton from either side of the uronic acid sugar ring presented us with a conundrum; the degradation of CS substrates could occur in the same manner as in chonAC, whereas the structure provided no clear indications how the same tetrad could be involved in abstracting the C-5 proton from the other side of the uronic acid ring during DS degradation.

The most straightforward way to identify catalytically essential residues is to determine the structure of the enzyme–substrate/inhibitor complex. Despite substantial efforts using multifaceted crystallization approaches we were not able to obtain crystals of such complexes for chonABC. Therefore, we decided to use a different structural approach to identify other catalytically important residues in addition to the tetrad. We searched for a distantly related member of the chonABC family aiming to determine its structure and, by comparison with PvulABCI, to identify structurally conserved constellations of residues in the proximity to the catalytic tetrad that could potentially be involved in catalysis of DS substrates. One such enzyme (BactnABC, 1014-amino-acid protein) with similar specificity as PvulABCI was identified in *Bacteroides thetaiotaomicron*, a prominent member of the human gut microbiota, containing a large contingent of proteins responsible for breaking down of the otherwise indigestible dietary oligosaccharides (Backhed et al. 2005) and has been partially characterized (Linn et al. 1983). BactnABC is only distantly related to PvulABCI (23% sequence identity); hence, we decided to investigate its crystal structure.

Comparing the structures of PvulABCI and BactnABC we identified two conserved histidines and an arginine in the substrate-binding cleft $\sim$12 Å from the putative catalytic tetrad. Using site-directed mutagenesis, we demonstrate that these histidines are essential only in DS degradation, whereas the arginine is required for catalysis of all substrates. Moreover, we demonstrate the involvement of the divalent metal cations Ca^{2+}/Mg^{2+} in the catalysis of DS substrates. Based on these observations we hypothesize that members of the chonABC family

271
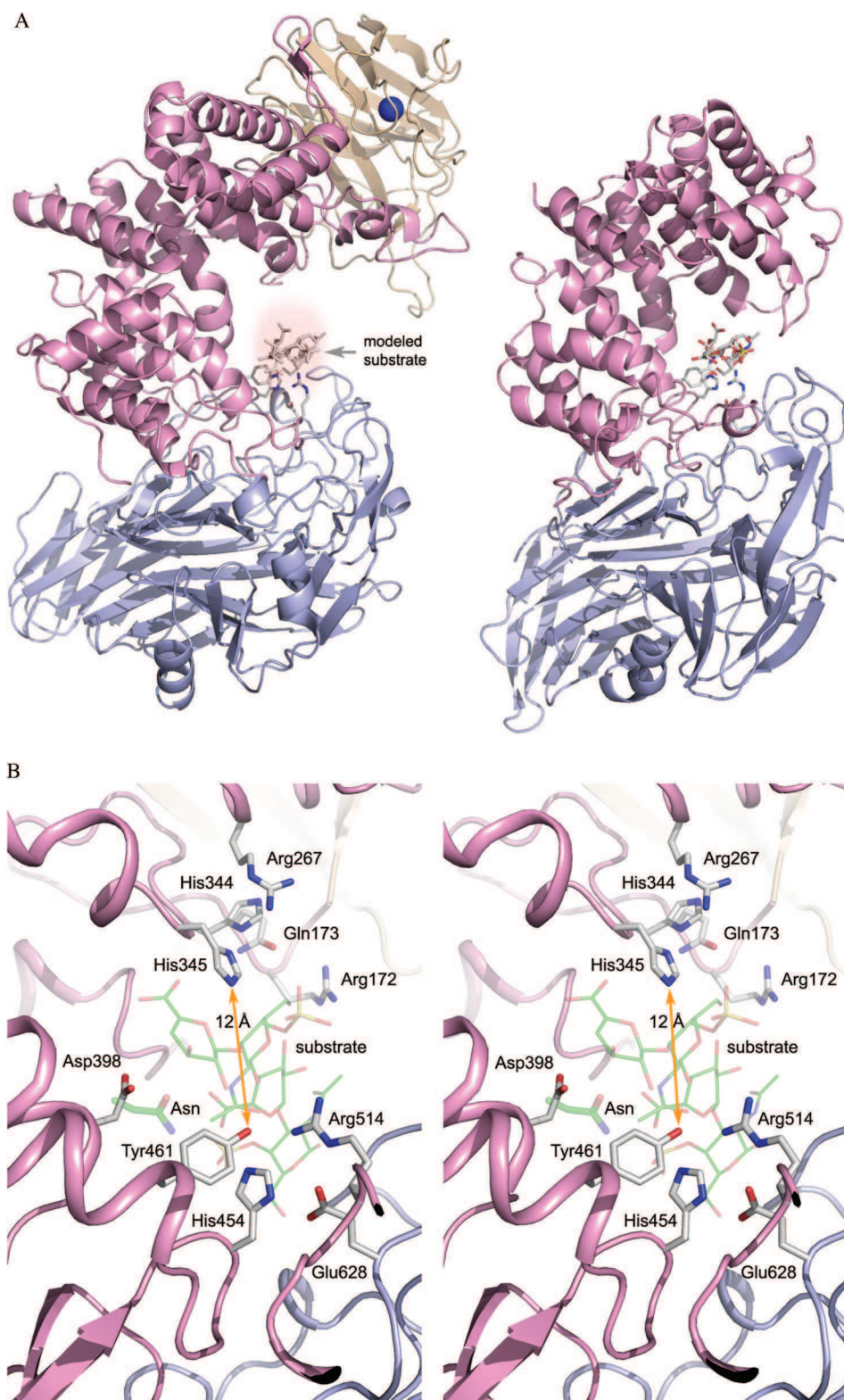
Fig. 2. The structure of BactnABC. (**A**) Left: a cartoon representation of a BactnABC monomer. Colors: N-terminal domain – wheat, middle domain – magenta, C-terminal domain – light blue, Ca^{2+} ion – blue sphere; the tetrad sidechains are shown in stick mode. The oligosaccharide substrate is modeled based on PedAC. Right: cartoon representation of PedAC with a bound tetrasaccharide IdoA(1→3)GalNAc4S(1→4)IdoA(1→3) GalNAc4S (where GalNAc4S stands for N-acetyl-D-galactosamine sulfated at carbon 4 and IdoA for α-L-iduronic acid). The substrate-binding cleft in BactnABC is much more open than that in PedAC. (**B**) Stereo view of the substrate-binding site of BactnABC with the sidechains of the tetrad and residues identified in this work shown as sticks. The modeled position of the substrate tetrasaccharide IdoA(1→3)GalNAc4S(1→4)IdoA(1→3) GalNAc4S is shown by thin lines. The location of the neutralizing asparagine in the structure of PedAC relative to the tetrad and substrate is marked with Asn. The distance between the residues of the two clusters is greater than 12 Å. Figures were created with the program PyMol (http://www.pymol.org).

contain a composite active site consisting of two sets of partially overlappingresidues that are involved in the cleavage of CS and DS, respectively.

Results and discussion

The three-dimensional structure of BactnABC

Remarkably, despite low sequence identity, the structure of BactnABC is highly similar to that of PvulABCI (Figure S1, supplementary data). A structure-based sequence alignment shows a sequence identity of only 23% for the two proteins. The root-mean-square deviation (rmsd) of Cα atoms for individual domains is in the range 1.1–1.45 Å, and the overall superposition shows a small difference in the orientation of N-terminal domains relative the rest of the molecules, suggesting some inter-domain flexibility.

Briefly, the N-terminal domain (residues Ala14–Asp170) contains 10 antiparallel β-strands arranged in a two-layered jellyroll β-sheet fold (Figure 2A) common to carbohydrate-binding modules found in such enzymes like endo 1,4-β-D-xylanases (Charnock et al. 2000) and cellulase (Carvalho et al. 2004). Such carbohydrate-binding proteins contain a structural Ca^{2+} ion located between the second and third β-strand. We have identified a Ca^{2+} ion in the equivalent location in BactnABC, hepta-coordinated by Ser 24, Glu26, Asp50, Ser56, and Asp161 (2.3–2.7 Å distances). The central domain (residues Ala171–Gln593) has a double-layered $(\alpha/\alpha)_5$ incomplete toroid fold. Despite no recognizable sequence similarity, this domain is structurally similar to the catalytic domains of chonAC from *P. heparinus* and *A. aurescens* (Lunin et al. 2004), hyaluronate lyases (Li et al. 2000), xanthan lyase (Hashimoto et al. 2003), alginate lyases (Yoon et al. 1999), and *P. heparinus* heparinase II (Shaya et al. 2006). The noticeable difference between BactnABC and the other proteins is a much more open substrate-binding cleft in the former (Figure 2A). The C-terminal domain (residues Gly594–Lys1014) contains a stack of four antiparallel β-sheets and contributes Glu628 to the catalytic tetrad.

Structural alignment of PedAC, ArthroAC, PvulABCI, and BactnABC shows that the Tyr-His-Arg-Glu catalytic tetrads of chonAC enzymes (His225, Tyr234, Arg288, and Glu653 in PedAC (Huang et al. 2001)) have counterparts in BactnABC (His454, Tyr461, Arg514, and Glu628, supplementary Figure S2) and in PvulABCI. Furthermore, both BactnABC and Pvul ABCI have wide substrate-binding clefts. On the rim of the substrate-binding cleft opposite to the tetrad we have identified three residues conserved between both chonABC enzymes, His 344, His 345, and Arg172, capable of participating in catalysis or substrate binding. In this region we also found two other conservatively replaced residues that could be involved in substrate binding, namely Gln173 and Arg267 in BactnABC (Tyr, Lys, respectively, in PvulABCI). Contribution of all these residues to the catalyzed reaction was investigated by site-directed mutagenesis.

Ca^{2+} and Mg^{2+} dependence of BactnABC activity

Of the two lyases specific for either CS or DS, the activity of chondroitinase AC is independent of metal ions (Huang et al. 2001), whereas that of chondroitinase B requires Ca^{2+} utilized for charge neutralization of the acidic group of iduronic acid

Table I. X-ray crystallographic data

Data collection	
Space group	$P6_3$
Cell dimensions (Å)	$a = 223.6$, $c = 112.6$
Wavelength (Å)	0.97233
Resolution range (Å)	44.62–2.85 (2.92–2.85)
Observed/unique reflections[a]	419,435/139,287
Average redundancy	3.1 (1.7)
Completeness (%)	94.8 (59.4)
Rsym[b]	0.063 (0.400)
Average $I/\sigma(I)$	20.6 (1.6)

Refinement statistics	
No. of reflections[c]	72,509 (3,102)
R-work[d]	0.220 (0.413)
R-free[d]	0.262 (0.464)
No. of atoms/average B-factor	
Protein	15,824/59.3
Solvent	67/40.7
Ions (Ca^{2+})	2/62.1
$PO_4{}^{2-}$	16∗5 = 80/73.3
Ramachandran plot	
Allowed (%)	99.2
Generously allowed (%)	0.6
Disallowed (%)	0.2
Root-mean-square deviation	
Bonds (Å)	0.02
Angles (degrees)	1.9

[a]The Friedel pairs were not merged.
[b]Rsym $= (\Sigma|I\,obs - I\,avg|)/\Sigma\,I avg$.
[c]Reflections used for refinement with merged Friedel pairs.
[d]R-work/free $= (\Sigma|Fo - Fc|)/\Sigma Fo$.

Table II. Ca^{2+}/Mg^{2+} influence upon the specific activity of BactnABC. All experiments were done in triplicate. The substrate was dissolved in 50 mM Tris–HCl, pH 7.6, and the reaction was monitored at 232 nm over 300 s at 37°C. One microgram of BactnABC was used in the experiment. The CS-A used is from BioCorp while DS and CS-C are from Sigma

	Specific activity (U mg^{-1} prot)		
Metal ion	CS-A	CS-C	DS
50 mM Tris–HCl	12.1 ± 0.4	6.8 ± 0.8	0.2 ± 0.1
+10 mM EDTA	n.d.[a]	n.d.	n.d.
+10 mM $CaCl_2$	25.3 ± 0.3	13.6 ± 0.8	4.3 ± 0.1
+20 mM $CaCl_2$	29.6 ± 0.2	12.6 ± 0.4	2.5 ± 0.1
+10 mM $MgCl_2$	38.2 ± 0.4	19.1 ± 0.8	5.2 ± 1.8

[a]n.d. – not detected.

(Michel et al. 2004). The effect of divalent cations on the activity of the recombinant C-5 epimer-nonspecific BactnABC is therefore of importance in understanding the mechanisms involved in catalysis and substrate recognition. We tested the effects of Ca^{2+} and Mg^{2+} in a Tris–HCl buffer at 37°C, the temperature of maximal activity, and pH 7.6, the pH optimum for this enzyme. The addition of these ions had a dramatically different effect on activity toward CS (glucuronic acid) and DS (iduronic acid). The specific activity for CS substrates increased only moderately (~2-fold) while an increase of ~25-fold was observed for DS (Table II). This suggests that the metal ions play a key role in charge neutralization of iduronic acid (as found for chonB, Michel et al. 2004) but are less important for the glucuronic acid epimer (as seen in chonAC, Pojasek et al. 2001; Lunin et al. 2004). No increase in activity was observed

for Mn^{2+} and Zn^{2+} (data not shown). Addition of 10 mM EDTA abolished the activity toward either substrate indicating that the presence of divalent cations is essential for BactnABC activity. No indication of a large structural change was found in the CD spectra upon the addition of EDTA (data not shown) making it unlikely that the lack of activity was caused by the removal of the structural Ca^{2+} from the N-terminal domain affecting indirectly the substrate-binding site.

Two overlapping catalytic sites reside within a single substrate-binding site

The β-elimination reaction mechanism requires neutralization of the negative charge of the uronic acid carboxylic group to reduce the pKa of the proton bound to C-5 (Gacesa 1987). Abstraction of this proton by a general-base-acting residue triggers the formation of a C-4–C-5 unsaturated bond in the uronic acid, accompanied by the elimination of the 4-linked hexosamine assisted by a general acid donating a proton to reconstitute the –OH of the leaving group.

The C-5 epimer-specific enzymes chonAC and chonB adopt completely different structures for stereoselective degradation of their respective substrates. ChonAC, with the $(\alpha/\alpha)_5$ helical toroid catalytic domain, neutralizes the acidic group of the glucuronate by two hydrogen bonds to an asparagine sidechain requiring its protonation and an additional hydrogen bond to a protonated histidine (Lunin et al. 2004). ChonB, on the other hand, has a right-handed β-helical fold and utilizes a Ca^{2+} ion coordinated between the protein sidechains and the acidic group of the iduronate for its neutralization (Michel et al. 2004). The residues playing the roles of general base and general acid also differ between these enzymes. Thus, chonAC uses a tyrosine for both functions while chonB utilizes a rather unusual Lys/Arg pair. A common feature, found in complexes of both these enzymes with their substrates, is that the sugar ring of the uronic acid assumes a higher energy-twisted conformation upon binding, making the degradation of the glycosidic bond an energetically more favorable event (Lunin et al. 2004; Michel et al. 2004).

BactnABC (and PvulABCI), which combines the activities of both of these enzymes, shares structural similarities with chonACs. However, it contains an additional domain at its N-terminus, and its substrate-binding cleft, within the central $(\alpha/\alpha)_5$ domain, is significantly wider than the corresponding cleft in ArthroAC and PedAC (Figure 2). While the Tyr-His-Arg-Glu tetrad is structurally conserved, the tryptophan residues stacking against the galactosamine rings of the substrate in chonACs have no counterparts in chonABCs. Moreover, the asparagine interacting with the acidic group of the glucuronate in chonACs is substituted in chonABCs by an aspartate (Asp398 in BactnABC) tilted away from the proposed binding site of the substrate.

The conservation of the tetrad residues and the effects of their mutation on PuvABCI activity (Prabhakar et al. 2005) strongly indicate their involvement in catalysis. As expected, replacing these residues in BactnABC by alanines led to inactivation of the enzyme against all substrates (Table III). Thus the presence of the tetrad would explain the cleavage of CS as described for chonAC (Lunin et al. 2004) but not DS, which is indeed an inhibitor of chonAC. Also, the manner by which the negative charge of the acidic group of uronic acid is neutralized, in chonABC, remains an open question.

Surprisingly, our results clearly show that while the activity toward CS increases only slightly in the presence of divalent metal cations, DS degradation is substantially enhanced in their presence (Table II). We postulate that a divalent metal cation (either Ca^{2+} or Mg^{2+}) binds together with the substrate coordinating the uronate acidic group, possibly assisted by Asp398, and participates particularly in the charge neutralization of the iduronate during DS degradation, paralleling chonB (Michel et al. 2004).

The residues participating in DS degradation (iduronic acid epimer) remained an open question. Other than the strong effect of Ca^{2+} on the activity toward DS, no other similarities between BactnABC and chonB are evident. Therefore, we compared the structures of BactnABC and PvulABCI in search of other structurally conserved residues in the vicinity of the substrate-binding site that might be involved in catalysis. As described above, we identified His344, His345, and Arg172 as well as two conservative replacements, Arg267 and Gln173, located within the substrate-binding cleft $\sim$12 Å from the tetrad (Figure 2B). These five residues were mutated individually to alanines and the activities of the mutants toward CS and DS were measured (Table III). The expression levels of these mutants and their behavior during purification were similar to that of the wild-type enzyme.

The H344A and H345A mutants show no detectable activity toward DS in the standard assay but still degrade CS, albeit with 10- to 30-fold lower k_{cat}/K_M (Table III). Incubating these mutants overnight with DS showed traces of disaccharide degradation products on HPLC analysis for the H344A mutant indicating residual activity, whereas no disaccharides were observed for the H345A mutant showing that it is indeed inactive (data not shown). His345 is thus the best candidate for the role of general base for DS substrates. The R172A showed no activity with any substrate, neither in the standard assay (Table III) nor during the overnight incubation. The two other mutations, Q173A and R267A, reduced the activity toward all substrates by a factor of $\sim$2–10, suggesting that they function in substrate binding or in maintaining the integrity of the active site.

The data recorded for the mutants show that the tetrad amino acids and the distal Arg172 are essential for catalysis of all substrates while the distal histidines are essential only for DS degradation. Thus, we suggest that the general base abstracting the C-5 proton from the glucuronic acid of CS is Tyr461 (as in the case of chonAC), or the nearby His454 (a tetrad component) (Figure 1), while the role of a general base for DS is performed by His345. The most likely general acid residue donating the proton to the bridging oxygen is Tyr461 (as suggested for chonAC). This residue would play the same role for both epimers, since the intermediate state for either epimer of uronic acid after the removal of the C-5 proton is the same. We hypothesize that Arg172 is involved in substrate binding in subsite +2 (GlcNAc), playing analogous role to the tryptophanes in chonAC, rather than directly in catalysis. Furthermore, the fact that both the tetrad and the cluster of newly identified residues affect all substrates argues for the presence of a single substrate-binding site with a composite active site made of partially overlapping amino acids specific either for CS or DS degradation. The formation of such a composite active site can only be accomplished by narrowing the substrate-binding cleft in the presence of the substrate.

Table III. Kinetic analysis of BactnABC and its mutants. Mutants of the tetrad residues are boxed. Mutants of the basic amino acids identified in the second site are marked in gray

Enzyme	CS-A[a]			CS-C[c]			DS[d]		
	K_M (μM)	k_{cat} (min^{-1})	k_{cat}/K_M (μM^{-1} min^{-1})	K_M (μM)	k_{cat} (min^{-1})	k_{cat}/K_M (μM^{-1} min^{-1})	K_M (μM)	k_{cat} (min^{-1})	k_{cat}/K_M (μM^{-1} min^{-1})
WT	67 ± 1	15,792 ± 240	235.7	33 ± 3	10,404 ± 38	315.27	61 ± 8	2,307 ± 190	37.8
H454A	n.d.[b]	n.d.	n.d.	n.d.	n.d.	n.d.	n.d.	n.d.	n.d.
Y461F	n.d.	n.d.	n.d.	n.d.	n.d.	n.d.	n.d.	n.d.	n.d.
R514A	n.d.	n.d.	n.d.	n.d.	n.d.	n.d.	n.d.	n.d.	n.d.
E628A	n.d.	n.d.	n.d.	n.d.	n.d.	n.d.	n.d.	n.d.	n.d.
R172A	n.d.	n.d.	n.d.	n.d.	n.d.	n.d.	n.d.	n.d.	n.d.
Q173A	102 ± 5	7,389 ± 164	72.4	50 ± 2	1,984 ± 5	39.7	71 ± 1	408 ± 7	5.7
R267A	109 ± 5	12,320 ± 80	113.0	98 ± 6	3,706 ± 61	37.8	71 ± 2	250 ± 14	3.5
H344A	202 ± 20	5,560 ± 28	27.5	134 ± 2	2,143 ± 172	16.0	n.d.	n.d.	n.d.
H345A	171 ± 13	3,828 ± 40	22.4	195 ± 19	1,852 ± 129	9.5	n.d.	n.d.	n.d.
H453A	38 ± 8	1,057 ± 62	27.8	20 ± 0.5	385 ± 14	19.3	44 ± 4	352 ± 0.2	8.0

Results are the mean ± S.D. for at least three experiments.
[a]1 mg CS-A from porcine trachea (Biocorp) in a 50 mM K-phosphate buffer, pH 7.6, measured for 300 s at 37°C using 0.5 μg of enzyme.
[b]n.d. – not detected.
[c]1 mg Cs-C from shark cartilage (Sigma) in a 50 mM K-phosphate buffer, pH 7.6, measured for 300 s at 37°C using 1.0 μg of enzyme.
[d]1 mg DS from porcine intestinal mucosa (Sigma) in a 50 mM K-phosphate buffer, pH 7.6, measured for 300 s at 37°C using 1.5 μg of enzyme.

Thus, combining a structural comparison of distantly related enzymes from the same family with mutagenesis of structurally conserved residues and their kinetic characterization led to uncovering of novel residues essential for catalysis and their different roles in processing the two epimers of uronic acid.

Materials and methods

Bacterial growth

The *B. thetaiotaomicron* strain WAL 2926 was obtained from the Korean Culture Center of Microorganisms (KCCM) and cultivated at 37°C in nutrient broth. *Escherichia coli* BL21(DE3) (EMD Biosciences, La Jolla, CA) and DL41(DE3) were maintained at 37°C in Luria broth supplemented with 100 μg mL^{-1} ampicillin (Ap) when appropriate.

Standard methods. Standard recombinant DNA procedures were performed according to Sambrook and Russel (2001). Genomic DNA of *B. thetaiotaomicron* and plasmid DNA were isolated using the G-spin Genomic DNA Extraction kit (iNtRON, Korea) and the QIAprep G-spin Miniprep Kit (Qiagen, Mississauga, Ontario) respectively, according to the manufacturers' procedures. Transformation of *E. coli* was performed according to the Novagene protocol. DNA amplifications by PCR were done using Taq polymerase, while BactnABC mutants were constructed using the QuickChange Site-Directed Mutagenesis Kit (Stratagene, Cedar Creek, TX) and the primers listed in supplementary Table S1. Mutations were verified by DNA sequencing.

Cloning of the chondroitin ABC lyase gene from Bacteroides genome

The gene coding for BactnABC was amplified by PCR from *B. thetaiotaomicron* WAL 2926 genomic DNA using primers constructed according to the published sequence BT3324 (Xu et al. 2003). The PCR fragment was subcloned into the pET22b vector. DNA sequencing revealed 64 nucleotide differences with the published sequence (gi:29348733, Xu et al. 2003) translating into 16 amino acid differences (Supplementary Table S2). These differences are probably related to strain differences between the WAL 2926 and the VPI-5482 isolates (NCBI deposited sequence).

Expression and purification of BactnABC

E. coli BL21(DE3) was transformed with the expression vector containing BactnABC. Bacteria were cultivated in a 1 L LB-Ap medium and grown at 37°C with aeration. At an OD$_{600}$ of 0.6–0.8 the cultures were transferred to 30°C for 30 min, induced with 1 mM IPTG and incubated for 4 h at 30°C with aeration. Selenomethionine (SeMet)-labeled protein was expressed in *E. coli* methionine auxotroph DL41(DE3) maintained in the LeMaster medium supplemented with 25 μg mL^{-1} L-SeMet (Hendrickson et al. 1990). Cultures were incubated for 12–16 h at room temperature in the medium after induction with 1 mM IPTG.

The cells were harvested by centrifugation at 6000 × *g* for 30 min at 4°C and the pellet was resuspended in a 25 mL binding buffer (50 mM K$_2$PO$_4$, pH 7.6, 400 mM NaCl, 10 mM imidazole, 5 mM β-mercaptoethanol (β-ME)). Cells were lysed by the addition of 0.25 μg mL^{-1} lysozyme followed by sonication. After ultracentrifugation the lysate was applied to a 1.5 mL DEAE-Sepharose (GE Healthcare, Baie d'Urfe, Quebec) column and the unbound protein was loaded onto a 3 mL Ni-NTA column (Qiagen). The column was washed by 50 column volumes of buffer (50 mM K$_2$PO$_4$, pH 7.6, 1.0 M NaCl, 10 mM imidazole, 5 mM β-ME) and bound His$_8$-BactnABC eluted with 50 mM K$_2$PO$_4$, pH 7.6, 200 mM NaCl, 300 mM imidazole, 5 mM β-ME. This eluate was diluted 3× with 10 mM K$_2$PO$_4$, pH 6 and loaded onto a pre-equilibrated Mono-S HR 10/10 column (GE Healthcare). The column was washed with 30 mL of 10 mM K$_2$PO$_4$, pH 6, 200 mM NaCl and the protein eluted by 200–500 mM NaCl gradient over 5 column volumes. Fractions-containing BactnABC were combined, concentrated on a Centricon YM-50 concentrator (Millipore Corporation, Billerica, MA) and applied to a HiLoad 16/60 Superdex 200 column (GE Healthcare), with 50 mM K$_2$PO$_4$, pH

7.2, 150 mM NaCl, 5 mM DTT as a running buffer. BactnABC-containing fractions were pooled and concentrated to 6–8 mg mL^{-1}. SeMet-labeled protein and BactnABC mutants were purified in the same manner.

Kinetic analysis and divalent cation requirement

Activity of BactnABC and its mutants was determined spectrophotometrically at 37°C using chondroitin-4-sulfate, CS-A (BioCorp), DS (Sigma, Oakville, Ontario), and chondroitin-6-sulfate, CS-C (Sigma) as substrates at concentrations of 0.1–5 mg mL^{-1} in a reaction buffer containing 50 mM K$_2$PO$_4$, pH 7.6. One microgram of BactnABC was added and initial reaction rates were monitored for 300 s following the absorbance at 232 nm. Kinetic parameters (k_{cat} and K_M) were determined using Hanes plots according to the equation: $[S]/v = K_m/V_m + [S]/V_m$. Data were interpreted using the program Hyper Version 1.0.0 (http://wvlc.uwaterloo.ca/biology447/modules/module7/hyper/index.htm). The molar absorption coefficient (ε) of 3800 M^{-1} cm^{-1} was used to calculate product release.

The influence of the divalent cations Ca^{2+}/Mg^{2+} on the activity of BactnABC was evaluated in a Tris–HCl buffer. The protein was dialyzed into 50 mM Tris–HCl, pH 7.6, and its specific activity against 1 mg of different substrates was measured as a function of CaCl$_2$ concentration. The experiment was repeated with addition of 10 mM EDTA and 10 mM MgCl$_2$.

Crystallization and data collection

Initial crystallization conditions were identified by hanging drop vapor diffusion at 20°C using the Index Screen (Hampton Research, Aliso Viego, CA). After optimization, the best crystals grew from 17% (w/v) PEG 3350, 0.2 M ammonium sulfate and 100 mM HEPES pH 6.50–7.00 at 4°C. These conditions were also used to produce crystals from SeMet-labeled protein. The crystals belong to the space group $P6_3$, with unit cell dimensions of $a = 223.4$ and $c = 112.6$ Å, and contain two molecules in the asymmetric unit with $V_M = 3.53$ Å^3 Da^{-1} (solvent contents 65%). For data collection the crystals were soaked at 4°C in mother liquor supplemented with 12% (w/v) glycerol, picked up in a nylon loop, and flash cooled in liquid N$_2$. Diffraction data extending to a 2.85 Å resolution were collected at the Se absorption peak ($\lambda = 0.97233$ Å) of ID22 beamline (APS) on a MAR CCD 300 mm area detector (MAR Research, Germany) set at a distance of 400 mm. Images were processed with the HKL2000 program (Otwinowski and Minor 1997).

Structure determination and refinement

The structure of BactnABC was solved by single-wavelength anomalous dispersion (SAD). A total of 70 selenium sites were located using the program SHELXD (Sheldrick 1991). The heavy atom sites were refined using SHARP (Bricogne et al. 2003). Solvent flattening with RESOLVE (Terwilliger 2002) yielded a figure-of-merit of 0.82. The model was built with COOT (Emsley and Cowtan 2004) and refined with REFMAC5 (Murshudov et al. 1997) against the SAD dataset, including the TLS option (the molecule was divided into three domains). A strong peak in the electron density was interpreted as a Ca^{2+} ion based on the ligand geometry and reasonable B-factors. Refinement at a 2.85 Å resolution converged with an R-factor of 0.220 and R-free of 0.262, with two SeMet-labeled monomers in the asymmetric unit consisting of residues Ala-14 to Lys-1014, one bound Ca^{2+} ion for each monomer, 16 phosphate ions, and 67 water molecules (Table I). Residues Ser558–Tyr567 are disordered and were not modeled. The final model has good geometry (PROCHECK; Laskowski et al. 1993). Coordinates have been deposited to the Protein Data Bank (Berman et al. 2000) with the code 2Q1F.

Supplementary Data

Supplementary data for this article is available online at www.glycob.oxfordjournals.org.

Conflict of interest statement

None declared.

Abbreviations

ArthroAC, *Arthrobacter aurescens* chondroitinase AC; BactnABC, *Bacteroides thetaiotaomicron* chondroitinase ABC; chonABC, chondroitinase ABC; chonAC, chondroitinase AC; chonB, chondroitinase B; CS, chondroitin sulfate; DS, dermatan sulfate; GAG, glycosaminoglycan; GalNAc, *N*-acetyl-D-galactosamine; GlcA, β-D-glucuronic acid; IdoA, α-L-iduronic acid; PedAC, *Pedobacter heparinus* chondroitinase AC; PvulABCI, *Proteus vulgaris* chondroitinase ABC I; SeMet, selenomethionine.

References

Allard ST, Giraud MF, Naismith JH. 2001. Epimerases: Structure, function and mechanism. Cell Mol Life Sci. 58:1650–1665.

Backhed F, Ley RE, Sonnenburg JL, Peterson DA, Gordon JI. 2005. Host-bacterial mutualism in the human intestine. Science. 307:1915–1920.

Bao X, Nishimura S, Mikami T, Yamada S, Itoh N, Sugahara K. 2004. Chondroitin sulfate/dermatan sulfate hybrid chains from embryonic pig brain, which contain a higher proportion of L-iduronic acid than those from adult pig brain, exhibit neuritogenic and growth factor binding activities. J Biol Chem. 279:9765–9776.

Berman HM, Westbrook J, Feng Z, Gilliland G, Bhat TN, Weissig H, Shindyalov IN, Bourne PE. 2000. The protein data bank. Nucleic Acids Res. 28:235–242.

Bernfield M, Gotte M, Park PW, Reizes O, Fitzgerald ML, Lincecum J, Zako M. 1999. Functions of cell surface heparan sulfate proteoglycans. Annu Rev Biochem. 68:729–777.

Bricogne G, Vonrhein C, Flensburg C, Schiltz M, Paciorek W. 2003. Generation, representation and flow of phase information in structure determination: Recent developments in and around SHARP 2.0. Acta Crystallogr, Sect D: Biol Crystallogr. 59:2023–2030.

Capila I, Wu Y, Rethwisch DW, Matte A, Cygler M, Linhardt RJ. 2002. Role of arginine 292 in the catalytic activity of chondroitin AC lyase from *Flavobacterium heparinum*. Biochim Biophys Acta. 1597:260–270.

Carvalho AL, Goyal A, Prates JA, Bolam DN, Gilbert HJ, Pires VM, Ferreira LM, Planas A, Romao MJ, Fontes CM. 2004. The family 11 carbohydrate-binding module of *Clostridium thermocellum* Lic26A-Cel5E accommodates beta-1,4- and beta-1,3-1,4-mixed linked glucans at a single binding site. J Biol Chem. 279:34785–34793.

Charnock SJ, Bolam DN, Turkenburg JP, Gilbert HJ, Ferreira LM, Davies GJ, Fontes CM. 2000. The X6 "thermostabilizing" domains of xylanases are carbohydrate-binding modules: Structure and biochemistry of the *Clostridium thermocellum* X6b domain. Biochemistry. 39:5013–5021.

D'Amore PA. 1990. Modes of FGF release in vivo and in vitro. Cancer Metastasis Rev. 9:227–238.

Emsley P, Cowtan K. 2004. Coot: Model-building tools for molecular graphics. Acta Crystallogr, Sect D: Biol Crystallogr. 60:2126–2132.

Ernst S, Langer R, Cooney CL, Sasisekharan R. 1995. Enzymatic degradation of glycosaminoglycans. Crit Rev Biochem Mol Biol. 30:387–444.

Féthière J, Eggimann B, Cygler M. 1999. Crystal structure of chondroitin AC lyase, a representative of a family of glycosaminoglycan degrading enzymes. J Mol Biol. 288:635–647.

Folkman J, Klagsbrun M. 1987. Angiogenic factors. Science. 235:442–447.

Gacesa P. 1987. Alginate-modifying enzymes. A proposed unified mechanism of action for the lyases and epimerases. FEBS Lett. 212:199–202.

Hamai A, Hashimoto N, Mochizuki H, Kato F, Makiguchi Y, Horie K, Suzuki S. 1997. Two distinct chondroitin sulfate ABC lyases. An endoeliminase yielding tetrasaccharides and an exoeliminase preferentially acting on oligosaccharides. J Biol Chem. 272:9123–9130.

Hashimoto W, Nankai H, Mikami B, Murata K. 2003. Crystal structure of *Bacillus* sp. GL1 xanthan lyase, which acts on the side chains of xanthan. J Biol Chem. 278:7663–7673.

Hendrickson WA, Horton JR, LeMaster DM. 1990. Selenomethionyl proteins produced for analysis by multiwavelength anomalous diffraction (MAD): A vehicle for direct determination of three-dimensional structure. EMBO J. 9:1665–1672.

Herron SR, Scavetta RD, Garrett M, Legner M, Jurnak F. 2003. Characterization and implications of Ca^{2+} binding to pectate lyase C. J Biol Chem. 278:12271–12277.

Huang W, Boju L, Tkalec L, Su H, Yang HO, Gunay NS, Linhardt RJ, Kim YS, Matte A, Cygler M. 2001. Active site of chondroitin AC lyase revealed by the structure of enzyme-oligosaccharide complexes and mutagenesis. Biochemistry. 40:2359–2372.

Huang W, Lunin VV, Li Y, Suzuki S, Sugiura N, Miyazono H, Cygler M. 2003. Crystal structure of *Proteus vulgaris* chondroitin sulfate ABC lyase I at 1.9 Å resolution. J Mol Biol. 328:623–634.

Huang W, Matte A, Li Y, Kim YS, Linhardt RJ, Su H, Cygler M. 1999. Crystal structure of chondroitinase B from *Flavobacterium heparinum* and its complex with a disaccharide product at 1.7 Å resolution. J Mol Biol. 294:1257–1269.

Lamzin VS, Dauter Z, Wilson KS. 1994. Dehydrogenation through the looking-glass. Nat Struct Biol. 1:281–282.

Lamzin VS, Dauter Z, Wilson KS. 1995. How nature deals with stereoisomers. Curr Opin Struct Biol. 5:830–836.

Laskowski RA, MacArthur MW, Moss DS, Thornton JM. 1993. PROCHECK: A program to check the stereochemical quality of protein structures. J Appl Crystallogr. 26:283–291.

Li S, Kelly SJ, Lamani E, Ferraroni M, Jedrzejas MJ. 2000. Structural basis of hyaluronan degradation by *Streptococcus pneumoniae* hyaluronate lyase. EMBO J. 19:1228–1240.

Linn S, Chan T, Lipeski L, Salyers AA. 1983. Isolation and characterization of two chondroitin lyases from *Bacteroides thetaiotaomicron*. J Bacteriol. 156:859–866.

Lunin VV, Li Y, Linhardt RJ, Miyazono H, Kyogashima M, Kaneko T, Bell AW, Cygler M. 2004. High resolution crystal structure of *Arthrobacter aurescens* chondroitin AC lyase: Enzyme-substrate complex defines the catalytic mechanism. J Mol Biol. 337:367–386.

Mattevi A, Vanoni MA, Todone F, Rizzi M, Teplyakov A, Coda A, Bolognesi M, Curti B. 1996. Crystal structure of D-amino acid oxidase: A case of active site mirror-image convergent evolution with flavocytochrome b2. Proc Natl Acad Sci USA. 93:7496–7501.

Michel G, Pojasek K, Li Y, Sulea T, Linhardt RJ, Raman R, Prabhakar V, Sasisekharan R, Cygler M. 2004. The structure of chondroitin B lyase complexed with glycosaminoglycan oligosaccharides unravels a calcium-dependent catalytic machinery. J Biol Chem. 279:32882–32896.

Murshudov GN, Vagin AA, Dodson EJ. 1997. Refinement of macromolecular structures by the maximum-likelihood method. Acta Crystallogr. D53:240–255.

Najmudin S, Andersen JT, Patkar SA, Borchert TV, Crout DH, Fulop V. 2003. Purification, crystallization and preliminary X-ray crystallographic studies on acetolactate decarboxylase. Acta Crystallogr, Sect D: Biol Crystallogr. 59:1073–1075.

Otwinowski Z, Minor W. 1997. Processing of X-ray diffraction data collected in oscillation mode. Methods Enzymol. 276:307–326.

Pawelek PD, Cheah J, Coulombe R, Macheroux P, Ghisla S, Vrielink A. 2000. The structure of L-amino acid oxidase reveals the substrate trajectory into an enantiomerically conserved active site. EMBO J. 19:4204–4215.

Pojasek K, Shriver Z, Kiley P, Venkataraman G, Sasisekharan R. 2001. Recombinant expression, purification, and kinetic characterization of chondroitinase AC and chondroitinase B from *Flavobacterium heparinum*. Biochem Biophys Res Commun. 286:343–351.

Prabhakar V, Capila I, Bosques CJ, Pojasek K, Sasisekharan R. 2005. Chondroitinase ABC I from *Proteus vulgaris*: Cloning, recombinant expression and active site identification. Biochem J. 386:103–112.

Rye CS, Matte A, Cygler M, Withers SG. 2006. An atypical approach identifies TYR234 as the key base catalyst in chondroitin AC lyase. Chem biochem. 7:631–637.

Sambrook J, Russell D. 2001. Molecular Cloning: A Laboratory Manual. . New York: Cold Spring Harbor Laboratory Press.

Shaya D, Tocilj A, Li Y, Myette J, Venkataraman G, Sasisekharan R, Cygler M. 2006. Crystal structure of heparinase II from *Pedobacter heparinus* and its complex with a disaccharide product. J Biol Chem. 281:15525–15535.

Sheldrick GM. 1991. Heavy atom location using SHELX-90. In: Wolf W, Evans PR, Leslie AG, editors. Isomorphous Replacement and Anomalous Scattering. Warrington: SERC Daresbury Laboratory. pp 80–86.

Tanner ME. 2002. Understanding nature's strategies for enzyme-catalyzed racemization and epimerization. Acc Chem Res. 35:237–246.

Terwilliger TC. 2002. Automated structure solution, density modification and model building. Acta Crystallogr, Sect D: Biol Crystallogr. 58:1937–1940.

Varki A. 1993. Biological roles of oligosaccharides: All of the theories are correct. Glycobiology. 3:97–130.

Vlodavsky I, Fuks Z, Ishai-Michaeli R, Bashkin P, Levi E, Korner G, Bar-Shavit R, Klagsbrun M. 1991. Extracellular matrix-resident basic fibroblast growth factor: Implication for the control of angiogenesis. J Cell Biochem. 45:167–176.

Xu J, Bjursell MK, Himrod J, Deng S, Carmichael LK, Chiang HC, Hooper LV, Gordon JI. 2003. A genomic view of the human-*Bacteroides thetaiotaomicron* symbiosis. Science. 299:2074–2076.

Yoon HJ, Mikami B, Hashimoto W, Murata K. 1999. Crystal structure of alginate lyase A1-III from *Sphingomonas* species A1 at 1.78 Å resolution. J Mol Biol. 290:505–514.